RSC Advances

PAPER

View Article Online
View Journal | View Issue

Cite this: *RSC Adv.*, 2020, **10**, 41197

Observation of glucose-6-phosphate anomeric exchange in real-time using dDNP hyperpolarised NMR†

Sivaranjan Uppala, Ayelet Gamliel, Gal Sapir, Jacob Sosna, J. Moshe Gomori and Rachel Katz-Brull *

Received 19th September 2020
Accepted 23rd October 2020

DOI: 10.1039/d0ra08022e

rsc.li/rsc-advances

A hyperpolarised-NMR acquisition approach that is sensitive to the process of glucose-6-phosphate anomerization is presented. Using selective depolarisation of one of the anomer's signals, it is possible to observe the replenishing of this signal due to the fast anomeric exchange of this compound. The forward to reverse reaction rate constants ratio was *ca.* 1.6.

The anomerization rate of glucose (Glc) intrigued researchers back at the turn of the 20th century.[1] Numerous studies into both Glc and glucose-6-phosphate (G6P) anomerization have been performed since,[2–15] due to their importance for the activities of anomer specific enzymes such as G6P dehydrogenase (which converts D-G6P to 6-phospho-D-glucono-1,5-lactone and is specific to β-G6P[2,16]), phosphoglucomutase (which converts G6P to G1P, and *vice versa*, and is specific to α-G6P[2]), and G6P isomerase (which interconverts G6P and fructose-6-phosphate (F6P) and is specific to α-G6P[2] and α-F6P[17]). G6P is the product of Glc phosphorylation which is carried out by hexokinases including glucokinase. From basic principles, the G6P anomer that is formed in this reaction is determined by the Glc anomer that serves as a precursor for this reaction.[2,14] Nevertheless, anomeric equilibrium of G6P will lead to the formation of the other G6P anomer, even if starting from a single Glc anomer (ESI, Scheme S1†). The Glc anomeric selectivity of hexokinase from different organisms and organs have been extensively studied and was found to depend on multiple variables such as temperature and the hexose concentration.[18–20] Recently, we have shown that yeast hexokinase shows selectivity for the β anomer of 2-deoxyglucose (2DG), a Glc derivative.[21] Additionally, we have shown that following the production of β-2DG-6-phosphate (β-2DG6P), anomeric equilibrium produces α-2DG6P.[21] Since G6P is a branch point for Glc metabolism and because G6P dehydrogenase, phosphoglucomutase, and G6P isomerase focus on different anomers of G6P, the anomerization of G6P is mechanistically important for the understanding of metabolic pathways routing.

However, the methodology for monitoring the anomerization process of the phosphorylated sugar is not trivial, specifically due to the speed of this process, which is at least two orders of magnitude faster than that of Glc.[2,3,22] In the 1960s, the methodologies for determining the anomeric conversion rates for Glc and G6P were indirect, for example necessitating a conversion to trimethylsilyl ethers for gas chromatography.[6,7] Other methods included calorimetry[2] and spectrophotometric measurements.[2,4,9,15] Later studies observed the two anomers of Glc and its derivatives using ^{1}H-,[6] ^{31}P-[5] and ^{13}C-nuclear magnetic resonance (NMR) in solution.

Simultaneous detection and differentiation between the anomers of Glc and G6P is done by ^{13}C NMR using the signals of the C_1 position. The C_1 signals of both anomers of are *ca.* 4 ppm apart and therefore can be resolved. Due to the low sensitivity of ^{13}C NMR, observing the anomerization process of sugars is challenging at thermal equilibrium, even when using ^{13}C-labeled compounds. Nevertheless, the two anomers have been observed *in vivo* in animal models[23] and in the human skeletal muscle[24] and brain.[25,26] However, using the C_1 signals it is typically not possible to discern between ^{13}C-labeled Glc and G6P *in vivo* due to the small chemical shift difference.

Mechanistic studies of Glc metabolism anomer specificity have typically used a specific anomer as a substrate. However, anomerization readily takes place as soon as the solid Glc or G6P are dissolved in water. At equilibrium, at 37 °C, a Glc solution contains 64% of the β and 36% of the α anomers. At 25 °C, the half-life for the anomeric exchange is 30–60 min (α to β and β to α, respectively),[3] and reports on the half-life in other temperatures vary.[27,28] Nevertheless, it is likely and generally assumed that at lower temperatures this half-life is longer. Therefore, experiments aiming at assessing the anomeric specificity of D-Glc metabolism were reported using low temperatures.[18] However, studies at lower temperatures affect enzyme activity. Another approach is to carry out the reaction in

Department of Radiology, Hadassah Medical Center, Hebrew University of Jerusalem, The Faculty of Medicine, Jerusalem, Israel. E-mail: rkb@hadassah.org.il

† Electronic supplementary information (ESI) available. See DOI: 10.1039/d0ra08022e

D_2O which was found to prolong the life time of the Glc anomers in solution.[7,12] However, D_2O may affect enzyme activities[14] due to H–D exchange of protein bound protons. In addition, the binding of Glc anomers was studied by saturation transfer difference NMR (STD NMR).[29]

We note that NMR methods that are based on ^{1}H detection *per se*, in the absence of isotopic label, whether direct or *via* chemical exchange saturation transfer (CEST)[30] cannot differentiate between Glc anomers. The transition states for the ring-opening and ring closing in the mutarotation reactions of Glc were studied by saturation transfer ^{13}C NMR,[31] and mutarotase activity on Glc[32] and on its sulfonated derivatives[33] were studied by ^{1}H and ^{13}C NMR exchange spectroscopy (EXSY) in one and two dimensions. Rate constants for anomerization of furanose sugars in D_2O were obtained by ^{1}H and ^{13}C saturation-transfer NMR spectroscopy[34] but the use of D_2O has been shown to slow down the anomerization of G6P.[4]

The dissolution-dynamic nuclear polarisation (dDNP) approach[35] has revolutionised the ability of NMR to monitor chemical and biochemical processes much faster and using physiologically relevant substrate concentrations. Furthermore, kinetic analysis through selective dDNP enhanced signal saturation or inversion has been reported.[36] Using the dDNP approach, the distribution of stable isotope-labelled Glc and its metabolites can be investigated at 3–4 orders of magnitude higher signal-to-noise ratio (SNR) compared to thermal equilibrium NMR spectroscopy studies.[21,37] [$^{13}C_6$,D_7]Glc has been utilised in several dDNP studies both as a metabolic agent[14,21,38–41] and as an imaging agent.[19,37] The labelling with ^{13}C is required for increasing the ^{13}C-NMR SNR. The deuteration of the ^{13}C sites (deuterium substitution of directly bound protons) is necessary to prolong the T_1 of these directly bound ^{13}C nuclei,[37,42] to enable observation of the hyperpolarised state and thus allow detection of chemical and enzymatic processes. Still, the lifetimes of the hyperpolarised sites of this stable-isotope labelled Glc analogue are relatively short, with T_1 relaxation times of about 10 to 20 s.[21] Therefore, this technique is suitable for investigation of fast processes, of the order of seconds. Although the C_1 positions of [$^{13}C_6$,D_7]Glc and [$^{13}C_6$,D_7]G6P anomers have been previously monitored in dDNP studies of hexokinase reactions,[13,21] their anomeric exchange rates were not characterised. Here we have devised a selective RF pulse excitation strategy and an experimental dDNP approach for monitoring the anomeric exchange of [$^{13}C_6$,D_7]G6P in real-time.

^{13}C-NMR of [$^{13}C_6$,D_7]Glc and [$^{13}C_6$,D_7]G6P offers a unique capability to observe both the α and β anomers of these compounds in solution. This is because for both these compounds the chemical shift difference between the $C_1\alpha$ and the $C_1\beta$ signals is large enough to be observed, even in the presence of the complex split signals due to the *J*-coupling with the adjacent ^{13}C and D nuclei.[21] Hyperpolarization of [$^{13}C_6$,D_7]Glc yields NMR signals that can be monitored with a temporal resolution of the order of seconds which is important when attempting to observe fast anomeric exchange processes. In addition, we have capitalised on the properties of a uniformly labelled compound in a hyperpolarised state, where there is a potential to quench one of the signals specifically. This is because the quenched signal cannot return to its starting level as the signal will relax to thermal equilibrium and the hyperpolarised signal is 3–4 orders of magnitude larger than that.

Our aim in this study was to null the signal of one of the anomers in a reaction mixture that contained both anomers in equilibrium and then observe and quantify the build-up of the nullified anomer signal as the anomeric equilibrium took place. It is important to note that nulling the signal of one of the anomers does not modify the reaction composition or the equilibrium process, but only the presentation in the NMR spectrum: the remaining hyperpolarised state in one of the anomers operates as a label, to highlight the formation of the other. To the best of our knowledge, this is the first investigation of anomeric exchange using hyperpolarised NMR.

First, we investigated this approach on hyperpolarised [$^{13}C_6$,D_7]Glc which was introduced into a hexokinase reaction medium, but without the enzyme. The following acquisition strategy was taken: first, a series of ten frequency selective RF pulses was applied to fully excite only the C_1 signal of the β anomer. The lower panel in ESI Fig. S1A† (time 1–10 s), demonstrates that indeed only this signal was excited and decayed quickly due to this massive depolarisation, it also demonstrates the need for the application of several selective pulses. Immediately after this selective depolarisation, a series of hard (non-selective) RF pulses was applied to excite the entire ^{13}C bandwidth with a low flip angle (10°). The resulting spectra displayed all of the expected hyperpolarised [$^{13}C_6$,D_7]Glc signals except for that of the $C_1\beta$ signal (which was depolarised by the previous selective pulse series). This result indicated that once depolarised, the $C_1\beta$ signal of hyperpolarised [$^{13}C_6$,D_7]Glc cannot regain its intensity, even though all of the other ^{13}C sites retain their hyperpolarised state. We note that we have specifically chosen to use formulations in which the starting material, [$^{13}C_6$,D_7]Glc, was already in anomeric equilibrium in order to monitor the solution composition at equilibrium (ESI Note S3,† Materials and methods, dDNP).

To validate this experimental approach and make sure that the application of the frequency selective RF pulses does not affect the decay of other hyperpolarised sites, we acquired hyperpolarised signals from a similar hyperpolarised solution of [$^{13}C_6$,D_7]Glc using only the series of non-selective, low flip-angle pulses. Indeed, all of the signals of hyperpolarised ^{13}C were observed (ESI Fig. S1B†) and appeared to decay at a similar decay rate (ESI Fig. S1C and Table S1†). This acquisition approach was further validated as described in the ESI S2.†

Next, we applied the same acquisition strategy (selective pulses on $C_1\beta$ followed by non-selective acquisition) on a hyperpolarised [$^{13}C_6$,D_7]Glc solution which was combined with a solution containing the enzyme hexokinase. This reaction led to a quick conversion of [$^{13}C_6$,D_7]Glc to [$^{13}C_6$,D_7]G6P, as confirmed by the immediate appearance of the C_6 signal of [$^{13}C_6$,D_7]G6P (Fig. 1A). As opposed to the experiment without the enzyme, a signal at the $C_1\beta$ chemical shift was observed as well, despite the preceding depolarisation of this signal by the selective RF pulses. However, both $C_1\beta$ and $C_1\alpha$ signals appeared at a relatively lower intensity compared to those of hyperpolarised [$^{13}C_6$,D_7]Glc which did not undergo an

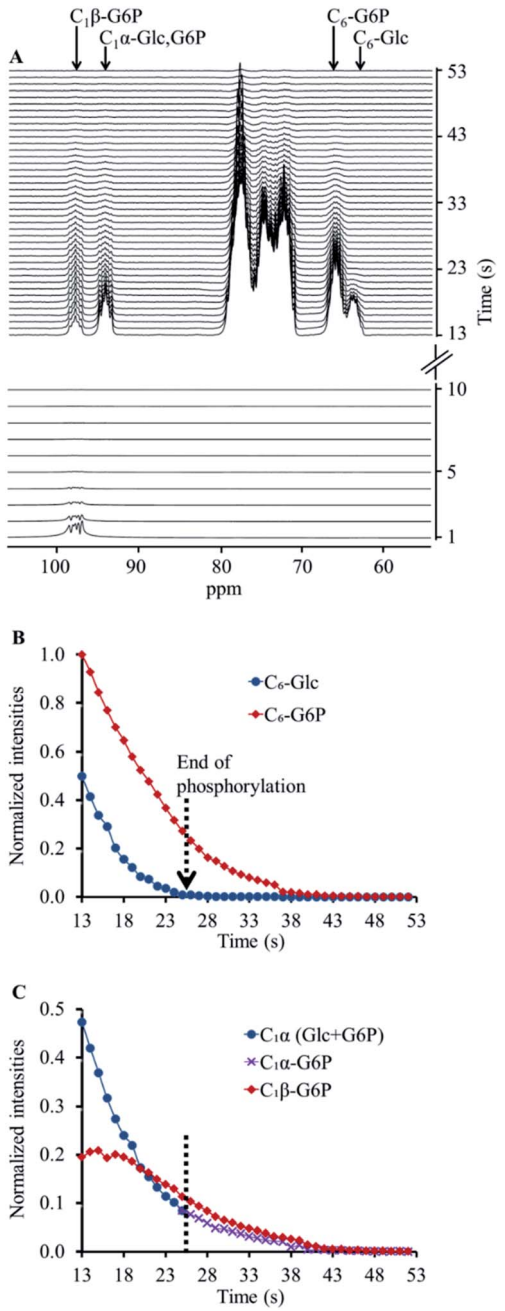

Fig. 1 Hyperpolarised [$^{13}C_6$,D_7]Glc in a reaction mixture with hexokinase (5.43 mg). (A) Lower panel, selective excitation and depolarisation of the $C_1\beta$ position for 10 s with a TR of 1 s. Upper panel, subsequent non-selective (hard pulse) excitations (from the 13th second) with the same TR. (B) A time course showing the signal decay for the chemical shifts of C_6-[$^{13}C_6$,D_7]Glc and C_6-[$^{13}C_6$,D_7]G6P determined using the non-selective excitations (upper panel in A). The dotted arrow indicates the time at which the phosphorylation reaction ended, as determined by the disappearance of the C_6-[$^{13}C_6$,D_7]Glc signal from the spectra. (C) A time course showing the signal decay for the chemical shifts of $C_1\alpha$ and $C_1\beta$ positions determined using the non-selective excitations (upper panel in A). The dotted arrow indicates the time at which the phosphorylation reaction ended (according to B). From this time onwards, the $C_1\alpha$ and $C_1\beta$ signals can be considered those of [$^{13}C_6$,D_7]G6P and were used in the analysis of [$^{13}C_6$,D_7]G6P anomeric exchange.

enzymatic reaction and did not undergo selective anomer depolarisation (Fig. S1B†). In the non-selective acquisition (Fig. 1A, upper panel), the signal of C_6 position showed a higher level of [$^{13}C_6$,D_7]G6P than [$^{13}C_6$,D_7]Glc already in the first spectrum. This suggested that a significant proportion of the reaction occurred during the application of the selective pulses. Because the anomeric exchange rate of G6P is higher than that of Glc[3] and because in the experiments without the enzyme the $C_1\beta$ signal was fully depolarised, it appeared likely that the $C_1\beta$ observed in this experiment is of [$^{13}C_6$,D_7]G6P and not of [$^{13}C_6$,D_7]Glc.

The appearance of hyperpolarised $C_1\beta$ signal in this experiment and the overall lower intensity of the C_1 position signals can be explained as follows. Hyperpolarised [$^{13}C_6$,D_7]Glc underwent phosphorylation during the application of the selective depolarizing pulses on $C_1\beta$. The $C_1\beta$ of [$^{13}C_6$,D_7]Glc and of the newly formed [$^{13}C_6$,D_7]G6P were continuously depolarised. Due to the anomeric equilibrium of [$^{13}C_6$,D_7]G6P, the signal of the $C_1\alpha$ position of [$^{13}C_6$,D_7]G6P was also affected as it exchanged with a depolarised position. In agreement, the signal of the $C_1\beta$ position of [$^{13}C_6$,D_7]G6P exchanged with a hyperpolarised position and therefore appeared in the spectra. Thus, this acquisition strategy appeared to be sensitive to the anomeric exchange of [$^{13}C_6$,D_7]G6P in real-time. Further testing and validation of this explanation is provided in ESI S3.†

The decay of the $C_1\alpha$ and $C_1\beta$ signals of [$^{13}C_6$,D_7]G6P in two enzymatic experiments (Fig. 1 and ESI S3†) is shown in ESI Fig. S4A and B,† respectively. These data served to determine the anomeric exchange rate of [$^{13}C_6$,D_7]G6P using a kinetic model previously developed to determine reaction rates of hyperpolarised substrates and products, whereas the respective NMR signals decay during the reaction according to each site's specific T_1.[43] Here, the $C_1\alpha$ was taken as the substrate and the anomeric exchange was taken as the reaction leading to $C_1\beta$ with a reaction rate constant $k_{forward}$. The reverse reaction, where $C_1\beta$ is converted back to $C_1\alpha$ was accounted for in the kinetic model with a reaction rate constant termed $k_{reverse}$. The T_1 of both compounds was fitted simultaneously with the forward and reverse reaction (anomeric exchange) rates. The intensities of $C_1\alpha$ and $C_1\beta$ signals of [$^{13}C_6$,D_7]G6P were taken from the time point at which entire [$^{13}C_6$,D_7]Glc pool was converted to [$^{13}C_6$,D_7]G6P. The results of the fit to the kinetic model are summarised in the ESI Table S2.†

In these experiments we have shown the ability to detect the anomeric exchange of [$^{13}C_6$,D_7]G6P in real-time. The dDNP hyperpolarisation technology provided the required orders of magnitude increase in SNR in order to be able to observe the process quickly and in concentrations that are physiologically relevant. In addition, the unique ability to quench the signal of one of the anomers enabled the direct observation of this process. For Glc, the time required to achieve complete equilibrium between the α and β anomers is a few hours.[7] Therefore, we could not observe this anomeric exchange process, as the hyperpolarised measurements can only take place while the hyperpolarised state of the site of interest exists. For [$^{13}C_6$,D_7]Glc ^{13}C sites, this time window was typically 30–50 s. However, as the G6P anomeric exchange rate is much faster,[2,3] observing

its anomeric exchange in real-time was possible using the current approach. For such a fast anomeric equilibrium the approach taken here was uniquely useful because it is much more challenging for observation with conventional assays.

As the anomeric equilibrium of both Glc and G6P has a preference for the β anomeric form,[3] we targeted here the exchange of the α to the β anomer (arbitrarily termed here as the forward reaction). To this end, the selective pulses were applied in the $C_1\beta$ frequency (98.6 ppm) and its signal was completely depolarised. Further consecutive acquisition with hard pulses enabled visualisation of the exchange of the $C_1\alpha$ position into $C_1\beta$, but only in the experiments where [$^{13}C_6$,D_7]G6P was formed and not on [$^{13}C_6$,D_7]Glc solutions without enzymatic activity.

On hyperpolarised ^{13}C spectra, the signals of [$^{13}C_6$,D_7]Glc and [$^{13}C_6$,D_7]G6P typically overlap, specifically because we could not use deuterium decoupling. Nevertheless, in a previous study, these C_1 signals were discerned using a careful deconvolution procedure.[21] Nevertheless, it is not trivial to discern the newly formed ^{13}C signals of [$^{13}C_6$,D_7]G6P in this type of spectra. To clearly and uniquely observe the anomerization and quantify the C_1-[$^{13}C_6$,D_7]G6P peak integrals we combined the selective depolarisation approach with a time window selection that was determined by monitoring the evolution of the C_6 position- for which the substrate ([$^{13}C_6$,D_7]Glc) and the product ([$^{13}C_6$,D_7]G6P) signals were resolved. The data used for determining the anomeric exchange process were taken only from those spectra that did not show the substrate signal, which suggested that the C_1 signals were due to G6P only.

As regards to the forward and reverse anomeric exchange rates (ESI Table S2†), it is interesting to note that the ratio of these rates was 1.64 ± 0.01 (n = 2). This ratio is in a good agreement with previous studies performed at thermal equilibrium on non-deuterated compounds.[3,5] However, the actual rates are not directly comparable due to differences in experimental conditions.[3,5] Because deuterium substitution may lead to an isotopic effect – *i.e.* an effect on metabolic and chemical exchange rates,[44] this agreement suggests that the results obtained here are relevant to non-labelled G6P as well. We believe that using the technique described here the anomerization of [$^{13}C_6$,D_7]G6P in other biological systems and models can be determined.

The T_1 of the C_1 position for the α and β anomers upon interaction with *ca.* 5 mg of the hexokinase enzyme was found to be 10 s (Table S2†). This determination is in agreement with the values determined previously on a similar reaction with a similar amount of enzyme, at the same magnetic field, but sampled with hard pulses only and analysed with a kinetic model that included the phosphorylation reaction rate and not the anomerization rate.[21] This strong similarity further validates the results of the kinetic model analysis done here. In addition, upon interaction with a higher enzyme content, the T_1 values decreased to *ca.* 7 s. This trend towards a decrease in T_1 upon interaction with the hexokinase enzyme was also observed previously for this reaction.[21] The use of a kinetic model that encompasses freedom for T_1 of the specific sites and simultaneous fit of the substrate and the product decay data enabled this determination of the anomerization exchange rate from the hyperpolarised data.

In conclusion, a methodology for observing the anomerization reaction of a stable-isotope labelled G6P in real-time and at physiological concentrations is presented. To the best of our knowledge, this is the first report in which the dDNP technology has been harnessed for researching anomerization reactions.

Conflicts of interest

There are no conflicts to declare.

Acknowledgements

The authors thank Dr Talia Harris for her assistance in the course of this study. This project has received funding from the European Union's Horizon 2020 Research and Innovation Program under grant agreement no. 667192, and from the Israel Innovation Authority, KAMIN Incentive program, grant agreement no. 63361.

References

1 T. M. Lowry, *J. Chem. Soc., Trans.*, 1903, **83**, 1314–1323.
2 M. Salas, E. Vinuela and A. Sols, *J. Biol. Chem.*, 1965, **240**, 561–568.
3 K. J. Schray and S. J. Benkovic, *Acc. Chem. Res.*, 1978, **11**, 136–141.
4 K. J. Schray and E. E. Howell, *Arch. Biochem. Biophys.*, 1978, **189**, 102–105.
5 R. S. Balaban and J. A. Ferretti, *Proc. Natl. Acad. Sci. U. S. A.*, 1983, **80**, 1241–1245.
6 C. Y. Lee, T. E. Acree and R. S. Shallenberger, *Carbohydr. Res.*, 1969, **9**, 356–360.
7 H. Jacin, J. M. Slanski and R. J. Moshy, *J. Chromatogr.*, 1968, **37**, 103–107.
8 B. Wurster and B. Hess, *FEBS Lett.*, 1974, **40**, S105–S111.
9 B. Wurster and B. Hess, *Eur. J. Biochem.*, 1973, **36**, 68–71.
10 C. Simmerling, T. Fox and P. A. Kollman, *J. Am. Chem. Soc.*, 1998, **120**, 5771–5782.
11 J. N. Brönsted and E. A. Guggenheim, *J. Am. Chem. Soc.*, 1927, **49**, 2554–2584.
12 W. J. Malaisse, I. Verbruggen, M. Biesemans and R. Willem, *Int. J. Mol. Med.*, 2004, **13**, 855–857.
13 E. Miclet, D. Abergel, A. Bornet, J. Milani, S. Jannin and G. Bodenhausen, *J. Phys. Chem. Lett.*, 2014, **5**, 3290–3295.
14 A. Sadet, M. M. Weber Emmanuelle, A. Jhajharia, D. Kurzbach, G. Bodenhausen, E. Miclet and D. Abergel, *Chem.–Eur. J.*, 2018, **24**, 5456–5461.
15 J. M. Bailey, P. H. Fishman and P. G. Pentchev, *Biochemistry*, 1970, **9**, 1189–1194.
16 J. E. Smith and E. Beutler, *Proc. Soc. Exp. Biol. Med.*, 1966, **122**, 671–673.
17 K. J. Schray, S. J. Benkovic, P. A. Benkovic and I. A. Rose, *J. Biol. Chem.*, 1973, **248**, 2219–2224.
18 W. J. Malaisse, *Adv. Biol. Chem.*, 2012, **2**, 1–9.

19 F. Fichaux, J. Marchand, B. Yaylali, V. Leclercq-Meyer, J. Catala and W. J. Malaisse, *Int. J. Pancreatol.*, 1991, **8**, 151–167.
20 V. Leclercq-Meyer, J. Marchand and W. J. Malaisse, *Horm. Metab. Res.*, 1991, **23**, 257–261.
21 G. Sapir, T. Harris, S. Uppala, A. Nardi-Schreiber, J. Sosna, J. M. Gomori and R. Katz-Brull, *Sci. Rep.*, 2019, **9**, 19683–19696.
22 J. M. Bailey, P. H. Fishman and P. G. Pentchev, *Biochemistry*, 1970, **9**, 1189–1194.
23 B. Künnecke, E. Küstermann and J. Seelig, *Magn. Reson. Med.*, 2000, **44**, 556–562.
24 R. Roussel, P. G. Carlier, C. Wary, G. Velho and G. Bloch, *Magn. Reson. Med.*, 1997, **37**, 821–824.
25 R. Gruetter, E. J. Novotny, S. D. Boulware, D. L. Rothman, G. F. Mason, G. I. Shulman, R. G. Shulman and W. V. Tamborlane, *Proc. Natl. Acad. Sci. U. S. A.*, 1992, **89**, 1109–1112.
26 B. Ross, A. Lin, K. Harris, P. Bhattacharya and B. Schweinsburg, *NMR Biomed.*, 2003, **16**, 358–369.
27 J. Okuda and I. Miwa, *J. Clin. Biochem. Nutr.*, 1986, **1**, 189–199.
28 W. J. Malaisse, M. H. Giroix, S. P. Dufrane, F. Malaisse-Lagae and A. Sener, *Biochim. Biophys. Acta*, 1985, **847**, 48–52.
29 A. Blume, M. Fitzen, A. J. Benie and T. Peters, *Carbohydr. Res.*, 2009, **344**, 1567–1574.
30 S. Walker-Samuel, R. Ramasawmy, F. Torrealdea, M. Rega, V. Rajkumar, S. P. Johnson, S. Richardson, M. Gonçalves, H. G. Parkes, E. Årstad, D. L. Thomas, R. B. Pedley, M. F. Lythgoe and X. Golay, *Nat. Med.*, 2013, **19**, 1067–1072.
31 B. E. Lewis, N. Choytun, V. L. Schramm and A. J. Bennet, *J. Am. Chem. Soc.*, 2006, **128**, 5049–5058.
32 P. W. Kuchel, B. T. Bulliman and B. E. Chapman, *Biophys. Chem.*, 1988, **32**, 89–95.
33 P. Abayakoon, J. P. Lingford, Y. Jin, C. Bengt, G. J. Davies, S. G. Yao, E. D. Goddard-Borger and S. J. Williams, *Biochem. J.*, 2018, **475**, 1371–1383.
34 A. S. Serianni, J. Pierce, S. G. Huang and R. Barker, *J. Am. Chem. Soc.*, 1982, **104**, 4037–4044.
35 J. H. Ardenkjaer-Larsen, B. Fridlund, A. Gram, G. Hansson, L. Hansson, M. H. Lerche, R. Servin, M. Thaning and K. Golman, *Proc. Natl. Acad. Sci. U. S. A.*, 2003, **100**, 10158–10163.
36 H. F. Zeng, Y. Lee and C. Hilty, *Anal. Chem.*, 2010, **82**, 8897–8902.
37 H. Allouche-Arnon, T. Wade, L. F. Waldner, V. N. Miller, J. M. Gomori, R. Katz-Brull and C. A. McKenzie, *Contrast Media Mol. Imaging*, 2013, **8**, 72–82.
38 T. Harris, H. Degani and L. Frydman, *NMR Biomed.*, 2013, **26**, 1831–1843.
39 S. Meier, M. Karlsson, P. R. Jensen, M. H. Lerche and J. O. Duus, *Mol. BioSyst.*, 2011, **7**, 2834–2836.
40 K. Kumagai, M. Akakabe, M. Tsuda, M. Tsuda, E. Fukushi, J. Kawabata, T. Abe and K. Ichikawa, *Biol. Pharm. Bull.*, 2014, **37**, 1416–1421.
41 K. N. Timm, J. Hartl, M. A. Keller, D. E. Hu, M. I. Kettunen, T. B. Rodrigues, M. Ralser and K. M. Brindle, *Magn. Reson. Med.*, 2015, **74**, 1543–1547.
42 H. Allouche-Arnon, M. H. Lerche, M. Karlsson, R. E. Lenkinski and R. Katz-Brull, *Contrast Media Mol. Imaging*, 2011, **6**, 499–506.
43 H. Allouche-Arnon, Y. Hovav, L. Friesen-Waldner, J. Sosna, J. Moshe Gomori, S. Vega and R. Katz-Brull, *NMR Biomed.*, 2014, **27**, 656–662.
44 C. E. Grimshaw and W. W. Cleland, *Biochemistry*, 1980, **19**, 3153–3157.